Hindawi
Shock and Vibration
Volume 2022, Article ID 4805589, 11 pages
https://doi.org/10.1155/2022/4805589

Research Article

Experimental Study on Dynamic Mechanical Characteristics and Energy Evolution of Sandstone under Cyclic Impact Loading

Xicai Gao ,[1,2] Huan Xia,[1,2] Xinyu Wang,[3] Cheng Zhao,[1,2] and Jianhui Yin[4]

[1] *Xi'an University of Science and Technology, State Key Laboratory of Coal Resources in Western China, Xi'an 710054, China*
[2] *Xi'an University of Science and Technology, Key Laboratory of Western Mine Exploitation and Hazard Prevention, Ministry of Education, Xi'an 710054, China*
[3] *School of Civil Engineering, Henan Polytechnic University, Jiaozuo 454000, China*
[4] *Shaanxi Coal and Chemical Industry Technology Research Institute Co., Ltd., Xi'an 710065, China*

Correspondence should be addressed to Xicai Gao; gxcai07@163.com

Received 26 September 2021; Accepted 6 January 2022; Published 19 January 2022

Academic Editor: Junyan Yi

In order to study the dynamic mechanical properties of the surrounding rock of roadway in deep mines with rock burst, cyclic impact compression tests of sandstone under different impact velocities were carried out by using the split Hopkinson pressure bar (SHPB) test system, and the dynamic stress-strain curves of the samples under cyclic impact loads and the relationship between energy dissipation and impact numbers were analyzed. The results show that, as the impact loading times increase, the initial elastic modulus of sandstone samples decreases, the peak stress decreases, and the peak strain increases; the average strain rate increases. The cumulative damage of sandstone samples under impact load is significantly affected by impact velocity and times. During the cyclic impact test, the reflected energy of sandstone increases with the increase of impact numbers, while the transmitted energy decreases and the absorbed energy increases; the cumulative specific energy absorption variable is introduced, and the cumulative specific energy absorption value of the samples increases with the increase of impact numbers, which can better characterize the variation of energy accumulation and dissipation of sandstone samples under cyclic impact.

1. Introduction

With the exhaustion of shall coal resources, more and more coal mines in China are turning to deep mining. Many coal mines in the northeast, north, east, central, and western regions are seriously threatened by rock burst. As mining goes deeper, the ground stress increases, and the risk of rock burst disasters and the number of mines subject to such disasters gradually rise [1–3]. During the mining process, the dynamic response of the coal and rock mass, the mining stress field, and the accumulation and release pattern of energy have all undergone significant changes. The experimental study on dynamic characteristics of instantaneous impact failure of underground rock mass provides an experimental basis for further understanding of the mechanism of rock burst and for the monitoring and early warning of dynamic disasters, which is of great significance to the production safety of coal mines.

In recent years, many scholars have conducted research on the dynamic response of the surrounding rock of deep roadways with rock burst, features of the disaster, prevention and control strategies, and support technology. Wu believes that different from ordinary roadways, roadways with rock burst are subjected to not only high static loads but also frequent impact loads [4]. The vibration velocity of the roadway surrounding rock is usually 0–10 m/s. Li and Gong studied the strength characteristics, fragmentation rules, and energy absorption efficiency of rocks under different combinations of dynamic and static loads [5–7]. Yang [8] studied the simulation experiments of marble under different blasting conditions and analyzed the mesocrack propagation and damage behavior of the rock damaged by blasting. Liu [9] analyzed the relationship between the wave curve, dynamic compressive strength, strength enhancement factor, specific energy absorption, and average strain rate of amphibolite samples under impact compression load through axial impact tests at different velocities. You et al. [10] conducted impact tests on salt rock under different confining pressures by using a separate SHPB test device with confining pressure and studied the dynamic mechanical properties and failure characteristics of salt rock based on the principle of energy dissipation; Yang et al. [11] took the common layered composite rock mass as the object and compared the stress wave propagation, dynamic stress-strain relationship, and energy dissipation rules of the composite rock mass at different impact velocities as the stress wave transmitted from hard to soft medium and from soft to hard medium. By considering the coupling effect of in situ stress and dynamic load of the rock mass in underground works, Jin et al. [12] carried out 3D dynamic compression tests on red sandstone and analyzed the variation of its average strain rate, dynamic peak stress, ultimate strain, and dynamic deformation modulus under different impact velocities and static stress conditions.

Current researches mostly focus on the dynamic response of rock or rock mass structure under a single impact. However, there are repeated dynamic loading processes in blasting excavation and hard rock formation induced cracking and in the surrounding rock of roadways with rock burst [13, 14]. Therefore, the study of the dynamic characteristics of sandstone under cyclic impact load is of great theoretical and practical significance for blast-induced cracking control and the stability of roadway surrounding rock [15]. Existing studies have generally found that the response parameters such as rock dynamic strength increase with the increase of loading and strain rate [16–20]. That is, the rock has obvious rate dependence. Wang et al. [21]and Luo et al. [22] analyzed the dynamic failure process of sandstone under cyclic impact load through numerical calculation method and laboratory experiment, and the dynamic deterioration characteristics and evolution laws of mesocracks are studied from both mesoscopic cracks and energy point of views. Gong et al. [23] investigated energy dissipation and particle size distribution of granite specimens under dynamic loads, using a conventional split Hopkinson pressure bar (SHPB) device with a high-speed camera. The above research results point out the direction of realizing the dynamic mechanical characteristics. In this study, an improved SHPB device is used to design the cyclic impact compression tests of sandstone at different impact velocities. Based on the stress-strain relationship, the dynamic mechanical properties and energy dissipation rules are analyzed. The research results are of certain significance for guiding actual project construction.

2. SHPB Tests

2.1. Sample Preparation. The test material was selected from the sandstone with a complete and uniform texture. According to the recommendations of the International Society for Rock Mechanics, the material was processed and polished into cylinders with a diameter and height of 100 mm, an end-face nonparallelism and non-perpendicularity less than 0.02 mm, and a deviation of end-face normal less than 0.25°. The sandstone samples are shown in Figure 1, and their static physical mechanics' parameters are shown in Table 1.

2.2. Test System. The SHPB test system improved by the Key Laboratory of Henan Polytechnic University is used in the tests. This system is mainly composed of air chamber, bullet, incident bar, transmission bar, buffer bar, data acquisition unit, and analysis unit. The incident bar, transmission bar, and absorption bar are made of 40Cr alloy steel, with a diameter of 100 mm, and a length of 5000 mm, 3000 mm, and 2000 mm, respectively, and the striker is a bar with a diameter of 100 mm and a length of 800 m. Its density is 7810 kg/m^3, longitudinal wave velocity is 5410 m/s, and elastic modulus is 210 GPa. At the same time, an ultrasonic parameter tester (ZT801) is used to test the wave velocity of the test samples before and after cyclic impact (see Figure 2).

2.3. Test Principles. Based on the assumption of one-dimensional stress wave and stress-strain uniformity, the dynamic stress, strain, and strain rate are calculated with the "three-wave method" [5] combined with the incident signal $\varepsilon_I(t)$, reflected signal $\varepsilon_R(t)$, and transmission signal $\varepsilon_T(t)$ collected by the strain gauge. The calculation formula is as follows:

$$\begin{aligned}
\sigma(t) &= \frac{A_0}{2A_S}E_0\left[\varepsilon_I(t)+\varepsilon_R(t)+\varepsilon_T(t)\right],\\
\varepsilon(t) &= \frac{C_0}{L_S}\int_0^t\left[\varepsilon_I(t)-\varepsilon_R(t)-\varepsilon_T(t)\right]\mathrm{d}t,\\
\dot{\varepsilon}(t) &= \frac{C_0}{L_s}\left[\varepsilon_I(t)-\varepsilon_R(t)-\varepsilon_T(t)\right],
\end{aligned} \tag{1}$$

where A_0 is the cross-sectional area of the pressure bar, E_0 is the elastic modulus of the pressure bar, C_0 is the longitudinal wave velocity of the pressure bar, L_0 is the length of the sample, and A_s is the cross-sectional area of the sample.

If the stress change in the sample is uniform without attenuation, $\varepsilon_I(t)+\varepsilon_R(t)=\varepsilon_T(t)$ can be obtained from the one-dimensional stress wave theory, and the above equation can be expressed by

$$\begin{aligned}
\sigma(t) &= \frac{A_0E_0}{A_S}\varepsilon_T(t),\\
\varepsilon(t) &= \frac{2C_0}{L_S}\int_0^t\left[\varepsilon_I(t)-\varepsilon_T(t)\right]\mathrm{d}t,\\
\dot{\varepsilon}(t) &= \frac{2C_0}{L_S}\left[\varepsilon_I(t)-\varepsilon_T(t)\right].
\end{aligned} \tag{2}$$

2.4. Test Plan. In order to explore the mechanical properties of sandstone under multiple disturbances from the surrounding rock of roadway with rock burst, the SHPB test system was used to conduct one-dimensional cyclic impact test on the sandstone. Before the test, the pressure bar was

Figure 1: Sandstone samples for impact tests.

Table 1: Static physical mechanics parameters of sandstone.

Density (kg/m^3)	2680
Compressive strength (MPa)	76.98
Elastic modulus (GPa)	15.84
Poisson's ratio	0.32

(a) (b)

Figure 2: SHPB test facility system and rock sonic velocimeter. (a) SHPB test facility and (b) rock sonic velocimeter.

first aligned for empty punching (no samples in place), and the air pressure was adjusted through multiple empty punching to stabilize the bullet velocity at a predetermined value. During the test, a brass sheet was placed between the bullet and the incident bar as a waveform shaper. The samples were placed between the incident bar and the transmission bar, and the bullet was applied to the contact surface of the samples and the pressure bar to reduce end-face friction. Constant-velocity cyclic impact test was conducted on the sandstone samples, each at a different impact velocity until the occurrence of macromechanical failure. The impact velocity was set to 6 m/s, 7 m/s, and 8 m/s, respectively. The impact velocity of the punch was controlled by adjusting the pressure value of the high-pressure air chamber and the initial position of the punch in the chamber, and the impact velocity was measured by a laser velocimeter. To ensure the reliability of the test, it is necessary to secure a dynamic stress equilibrium at both ends of the rock samples. The curves of dynamic stress equilibrium are shown in Figure 3, where σ_i, σ_r, and σ_t, respectively, represent the incident, reflection, and transmission stress of the bar. The sum of the incident wave and the reflected wave is basically the same as the transmitted wave, indicating that both ends of the rock sample are basically in a state of stress equilibrium during the test [3], which proves the validity of the test.

3. Dynamic Mechanical Characteristics of the Sandstone

The uniaxial cyclic impact test was carried out on the sandstone samples, and the impact velocity was set to approximately 6 m/s, 7 m/s, and 8 m/s. The main test results are shown in Table 2.

3.1. Dynamic Behavior of the Sandstone. The stress-strain curves of the sandstone samples under cyclic impact are shown in Figure 4. As the impact numbers increase, the peak stress of the sandstone samples decreases, and the strain

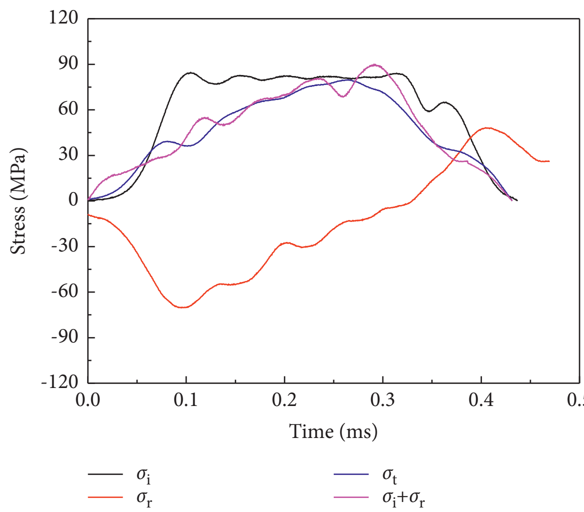

Figure 3: Dynamic stress equilibrium of sandstone.

Table 2: Experimental results of sandstone under cyclic impact loads.

No.	L_0 (mm)	D_0 (mm)	ρ (kg/m^3)	n	v (m/s)	P_v (m/s)	σ^f	ε^f	$\dot{\varepsilon}$/s^{-1}
				0	—	2950	—	—	—
				1	5.998	2717	79.78	0.0054	13.58
				2	—	2667	76.55	0.0053	13.41
				3	6.035	2587	75.29	0.0058	14.65
s0-2	100.04	100.68	2394.799	4	6.008	2584	75.07	0.0053	13.03
				5	5.957	2541	70.23	0.0053	13.19
				6	5.911	2481	70.81	0.0056	13.99
				7	—	2448	64.58	0.0059	14.72
				8	5.710	2427	61.11	0.0060	15.06
				0	—	2886	—	—	—
				1	—	2699	91.61	0.0057	15.21
				2	—	2625	89.49	0.0067	17.10
s0-1	100.13	100.66	2404.942	3	6.742	2551	87.64	0.0065	17.85
				4	7.080	2466	82.60	0.0068	16.89
				5	6.885	2375	76.31	0.0064	16.99
				6	7.290	—	69.45	0.0093	23.37
				0	—	2946	—	—	—
s0-6	99.97	100.89	2387.611	1	—	2688	121.62	0.0060	14.10
				2	—	—	106.33	0.0067	19.25

Notes: L_0 is the sample length; D_0 is the sample diameter; ρ is the sample density; P_v is the impact air pressure; n is the impact numbers; v is the measured impact velocity; σ^f is the peak stress; ε^f is the peak strain; $\dot{\varepsilon}$ is the average strain rate.

increases. The stress-strain curves overlapped during the first several impacts. The original defects such as microcracks and voids in the samples cause stress concentration. Cracks develop under the impact load, resulting in reduced capacity of load transfer inside the rock structure. With the increase of impact numbers, the slope of the initial elastic rise stage of the stress-strain curve gradually decreases, which means that the elastic modulus gradually decreases, and the mechanical properties of the rock samples continuously decline. With the increase of the impact velocity, the total impact numbers required for rock failure decrease. At the impact velocity of 6 m/s and 7 m/s, the internal cracks of the rock samples keep closing and opening under multiple impacts. The cumulative damage of the samples increases, resulting in the final failure of the samples. At an impact velocity of 8 m/s, the first impact caused too much damage to the samples, which exceeds their failure threshold. After the second impact, the samples are completely destroyed.

Figure 5 shows the relationship between the average strain rate of sandstone and the impact numbers under cyclic impact loading. It can be seen that during cyclic impact loading, the higher the impact velocity, the less the total impact numbers required for sandstone failure. The average strain rate of the sandstone samples at three impact velocities all shows an upward trend with the increase of impact numbers. When the impact numbers reach a certain

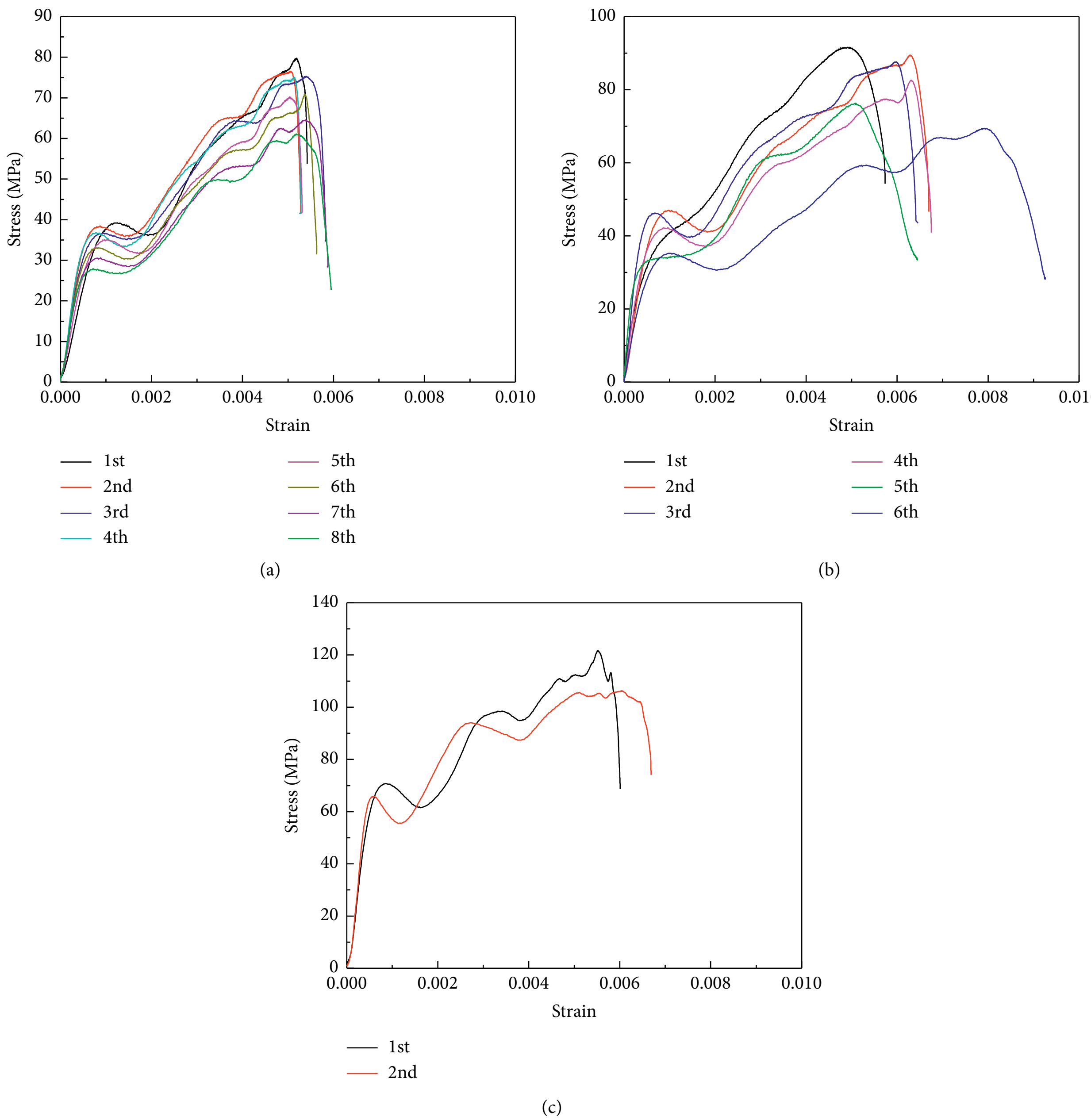

Figure 4: Stress-strain curves of sandstone under cyclic impact loads. (a) 6 m/s. (b) 7 m/s. (c) 8 m/s.

number, the samples are severely damaged and deformed inside, resulting in a sudden increase in the average strain rate.

Figure 6 shows the relationship between the peak strain of the sandstone and the impact numbers under cyclic impact at three velocities. It is clearly demonstrated that the peak strain of the sandstone samples rises with the increase of impact numbers. When the impact velocity is 7 m/s, the peak strain (ε^f) of the samples increases significantly after the second impact and then presents an alternating trend with the increase of impact numbers. The peak strain at the sixth impact increases more than that at the fifth time.

Figure 7 shows the relationship between the peak stress of the sandstone and the impact numbers under cyclic impact at three velocities. The peak stress of the sandstone samples shows a downward trend with the increase of impact numbers. At an impact velocity of 6 m/s, the peak stress of the sandstone rebounds slightly after the sixth impact and then rapidly declines. At an impact velocity of 7 m/s, the peak stress of the sandstone samples first decreases slowly and then decreases sharply with the increase of impact numbers. This is because, after each impact load, part of the energy goes to aggravate the damage of the samples. As the impact numbers continue to increase, more microcracks are generated inside the sandstone samples. The accumulation of the internal damage leads to reduced bearing capacity and increased deformation and average strain rate of the sandstone. After a certain impact number, the peak stress of the sandstone suddenly drops.

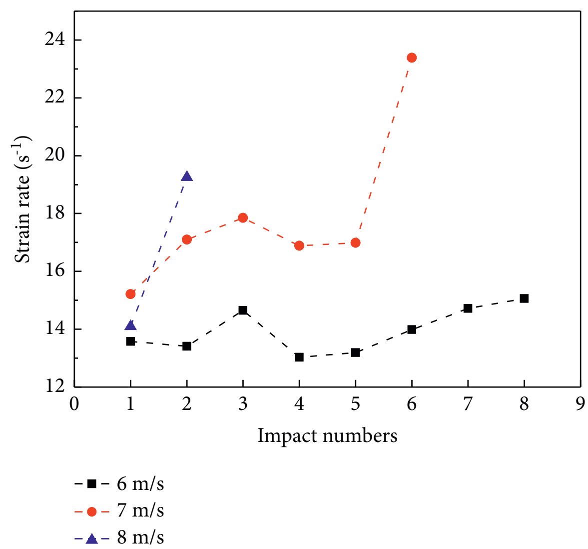

Figure 5: Average strain rate with the increase of impact numbers under different impact velocities.

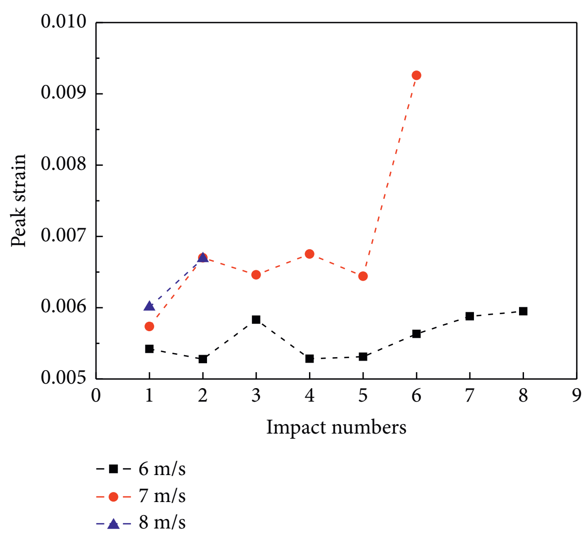

Figure 6: Peak strain with the increase of impact numbers under different impact velocities.

3.2. Failure Modes of Sandstone Samples. Table 3 shows the failure modes of sandstone samples under cyclic impact at different impact velocities. With the increase of the impact velocity, the fragment size of the sandstone samples decreases, and the number of fragments increases; the greater the impact velocity is, the earlier the macrocracks appear in the samples, and the less impact numbers are required from the appearance of macrocracks to failure.

At an impact velocity of 6 m/s, macrocracks appear after the fifth impact and failure occurs after the eighth impact; at 7 m/s, macrocracks appear after the fourth impact, and failure occurs after the sixth impact; at 8 m/s, no obvious macrocracks appear after the first impact while failure occurs after the second impact.

3.3. Damage Evolution. Figure 8 shows the variation of wave velocity of the sandstone samples with the impact numbers during the cyclic impact. After the first impact, the wave velocity of the sandstone samples decreases significantly, indicating that large cracks or damage has appeared inside the samples. With the increase of impact numbers, the wave velocity of the samples continues to decrease, and the damage inside the samples keeps expanding.

In order to study the damage evolution characteristics of rock, the macroscopic characteristic quantities such as density, elastic modulus, yield stress, and longitudinal wave velocity are usually used to characterize the damage degree of rock. At present, the method of defining rock damage variables by longitudinal wave velocity has been widely used

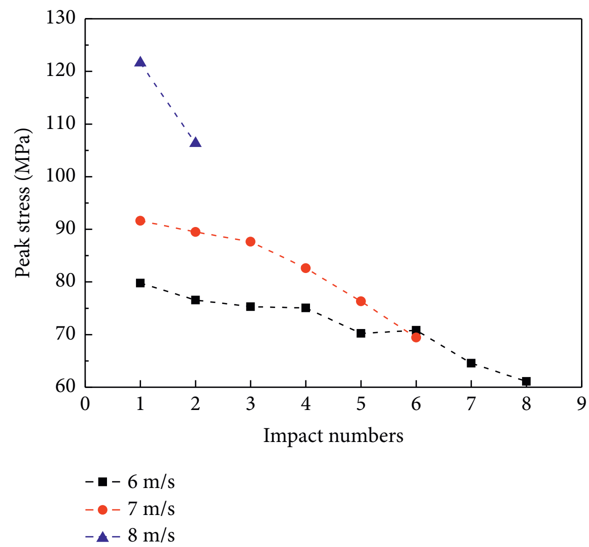

FIGURE 7: Peak stress with the increase of impact numbers under different impact velocities.

TABLE 3: Failure modes of sandstone samples.

Impact velocity (m/s)	Failure modes				
6	 $n=4$	 $n=5$	 $n=6$	 $n=7$	 $n=8$
7	 $n=3$	 $n=4$	 $n=5$		
8	 $n=1$	 0 $n=2$			

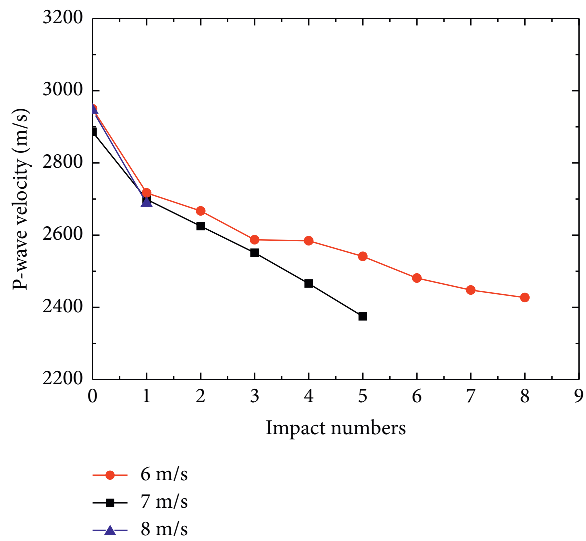

Figure 8: Relationships between P-wave velocity and impact numbers with different impact velocities.

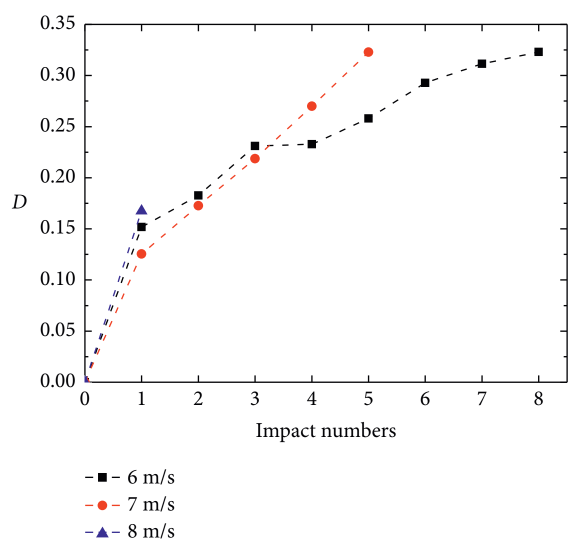

Figure 9: Relationships between rock damage and impact numbers with different impact velocities.

in indoor tests and field detection and achieved good results. The longitudinal wave velocity of rock materials is less affected by the conventional external environment. Therefore, rock materials can be used to reveal the damage evolution process of rock.

If the rock is regarded as an isotropic body composed of itself and its internal fractures, then based on the correlation between the longitudinal wave velocity of the material and the elastic modulus obtained from the wave theory, the damage variable defined by the longitudinal wave velocity can be expressed as follows:

$$D_n = 1 - \frac{v^2}{v_0^2}, \tag{3}$$

where D_n is the damage degree, v_0 is the acoustic wave velocity in the initial state of the material, and v is the longitudinal wave velocity of the sandstone samples after impact load.

Figure 9 shows the relationship between the damage degree of the sandstone samples and the impact numbers. It can be known that the cumulative damage of the sandstone samples under impact load is greatly affected by the impact velocity. When the impact velocity is small, the relationship curve between the damage degree and the impact numbers is relatively gentle. The greater the impact velocity, the more obvious the aggravation of damage is with the impact numbers. After the first impact, the damage degree of the sandstone samples increases sharply, which also indicates that the first impact contributes more to the damage of the samples. At this time, the inside of the samples has cracks developed or propagated.

4. Energy Evolution

According to the experimental loading principle of SHPB and the law of energy conservation, different kinds of energy are calculated by the following formulas using the strain curves of the incident wave, reflected wave, and transmitted wave:

$$\begin{aligned} W_I &= \frac{A_0 C_0}{E} \int \sigma_I^2 \mathrm{d}t \\ &= A_0 C_0 E \int \varepsilon_I^2 \mathrm{d}t, \\ W_R &= \frac{A_0 C_0}{E} \int \sigma_R^2 \mathrm{d}t \\ &= A_0 C_0 E \int \varepsilon_R^2 \mathrm{d}t, \\ W_T &= \frac{A_0 C_0}{E} \int \sigma_T^2 \mathrm{d}t \\ &= A_0 C_0 E \int \varepsilon_T^2 \mathrm{d}t, \\ W_S &= W_I - W_R - W_T, \\ E_V &= \frac{W_S}{V_S}, \end{aligned} \tag{4}$$

where W_I, W_R, W_T, and W_S are the incident energy, reflected energy, transmitted energy, and absorbed energy of the samples during the impact loading, V_S is the volume of the samples, and E_V is the absorbed energy per unit volume.

Figure 10 shows the relationship between the incident energy, reflected energy, transmitted energy, and absorbed energy of the samples under constant-velocity cyclic impact and impact numbers. It can be seen from the figure that the incident energy oscillates slightly as the impact is loaded more times. This is because, in the cyclic impact process, the impact air pressure is unstable, which results in a slight deviation in the velocity of each impact, and thus oscillation of the incident energy. A more stable incident energy means a smaller difference in impact velocity. With the increase of impact numbers, the reflected energy increases, the transmitted energy decreases, and the absorbed energy increases. When the sandstone samples have severe internal damage, the absorbed energy will also decrease. For example, at an impact velocity of 7 m/s, after the fifth impact, longitudinal cracks have appeared on the surface of the samples, and some cracks have also appeared on the edge, indicating serious internal damage to the samples. In this case, if the impact continues, the samples will be severely damaged, and the absorbed energy will gradually decrease. Most of the energy is released in the form of reflected energy. With the increase of impact numbers, the energy dissipation inside the samples is also constantly changing. In other words, the reflected energy increases and transmitted energy decreases, and the absorbed energy keeps increasing for the formation

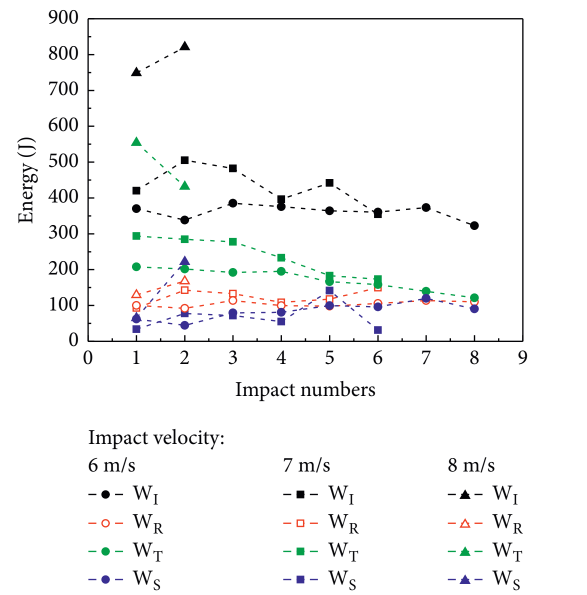

Figure 10: Variation of different kinds of energy with impact numbers.

and propagation of rock cracks. When the internal damage of the rock reaches a certain level, the samples will undergo tensile failure.

Figure 11 shows the variation of the absorbed energy per unit volume of the sandstone samples with the impact numbers under constant-velocity cyclic impact. It can be seen that the absorbed energy per unit volume rises and falls significantly with the increase of impact numbers. When the internal damage of the samples is serious, with the increase of impact numbers, most of the energy is released in the form of reflected energy, while less energy is absorbed by the samples. As a result, the absorbed energy per unit volume tends to decrease. For example, at an impact velocity of 7 m/s, obvious cracks appear on the surface of the samples after the fifth impact, which results in the absorption of more energy for the initiation and propagation of cracks in the samples during the impact. This further leads to a significant rise in the absorbed energy per unit volume. In the sixth impact, a small amount of energy absorbed by the samples is sufficient to cause failure.

In order to explore the variation of energy accumulation of the sandstone samples under cyclic impact loading, the cumulative specific energy absorption value is introduced, which is defined as the cumulative energy absorbed per unit volume of the samples during cyclic impact. The cumulative specific energy is calculated as follows:

$$\delta = \sum_{i=1}^{n} E_{V(i)}, \tag{5}$$

where δ cumulative specific energy absorption, n is the number of cyclic impact, and E_v is the energy absorbed per unit volume.

Figure 12 shows the relationship between the cumulative specific energy absorption value of the samples and the impact numbers. At the same impact velocity, the

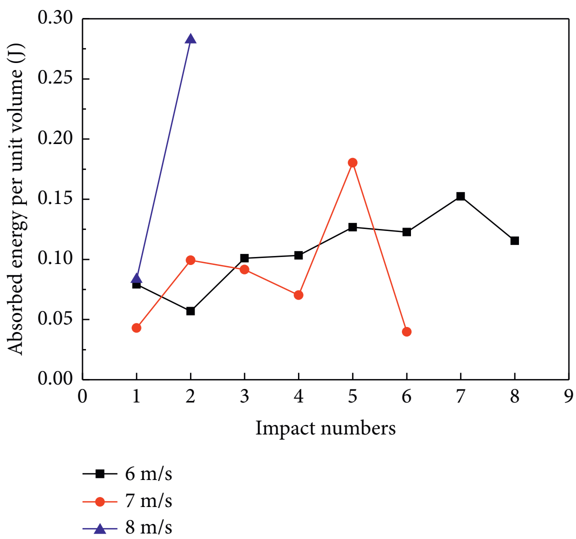

Figure 11: Variation of sandstone absorbed energy per unit volume along with impact numbers.

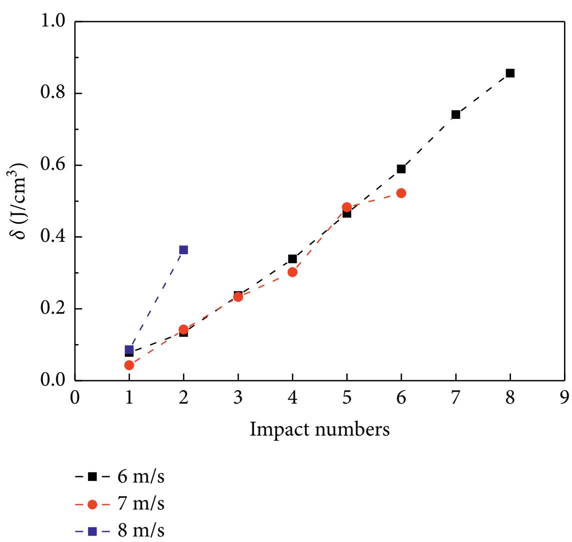

Figure 12: Relationships between δ and impact numbers under different impact velocities.

cumulative specific energy absorption value of the sample increases with the increase of impact numbers. During cyclic impact, the internal damage of the sample is cumulated, and the energy absorbed by the samples is stored in the form of elastic potential energy. When the elastic potential energy accumulates up to the threshold of stored energy, the elastic potential energy inside the samples is released, which leads to the continuous expansion of the microcracks inside the samples, increase of the fracture surface area per unit volume of the samples, and increase of the cumulative specific energy.

5. Conclusions

(1) Under uniaxial cyclic impact loading, as the impact numbers increase, the slope of the stress-strain curve of the sandstone samples in the initial elastic rising stage decreases, the peak stress decreases, and the peak strain increases; the average strain rate of the sandstone samples shows an overall upward trend with the increase of impact numbers; with the continuous increase of impact velocity, the total number of impact numbers required for sandstone failure decreases, the fragment size is smaller, and the number of fragments is larger.

(2) The ultrasonic wave velocimeter is used to calculate the damage degree of sandstone during the cyclic impact test. The cumulative damage of the sandstone samples is greatly affected by the impact velocity and the impact numbers. When the impact velocity is low, the relationship curve between the damage degree and the impact numbers is relatively gentle. With the increase of impact numbers, the damage degree increases dramatically.

(3) During the cyclic impact test, the energy absorbed by the samples is stored inside them in the form of elastic potential energy. With the increase of impact numbers, the reflected energy increases, while the transmitted energy decreases. The initiation and propagation of rock cracks are characterized by the continuous increase of the absorbed energy and the significant decrease of the absorbed energy per unit volume as the impact numbers increase. The cumulative specific energy absorption value is introduced. The cumulative specific energy absorption value of the samples increases with the increase of impact numbers, which can better characterize the variation of energy accumulation of the sandstone samples.

Data Availability

The data generated and analyzed in this manuscript are available from the corresponding author on reasonable request.

Conflicts of Interest

The authors declare that there are no conflicts of interest regarding the publication of this study.

Acknowledgments

This research was supported by the Natural Science Basic Research Program of Shaanxi (no. 2021JLM-10), the Natural Science Basic Research Program of Shandong (no. 2019JZZY020326), and the Open Fund of State Key Laboratory of Coal Resources in Western China, Xi'an University of Science and Technology (no. SKLCRKF1905). These financial supports are gratefully acknowledged.

References

[1] G. Z. Yin, X. Li, J. Lu, and M. Li, "Disaster-causing mechanism of compound dynamic disaster in deep mining under static and dynamic load conditions," *Journal of China Coal Society*, vol. 42, no. 9, pp. 2316–2326, 2017.

[2] E. Y. Wang, J. J. Feng, Q. M. Zhang, X. Kong, and X. Liu, "Mechanism of rock burst under stress wave in mining space," *Journal of China Coal Society*, vol. 45, no. 1, pp. 100–110, 2020.

[3] P. Wang, T. Yin, X. Li, S. Zhang, and L. Bai, "Dynamic properties of thermally treated granite subjected to cyclic impact loading," *Rock Mechanics and Rock Engineering*, vol. 52, no. 4, pp. 991–1010, 2019.

[4] Y. Wu, J. CHen, J. Jiao, Y. Zheng, and J. He, "Damage and failure mechanism of anchored surrounding rock with impact loading," *Journal of China Coal Society*, vol. 43, no. 9, pp. 2389–2397, 2018.

[5] X. B. Li, T. S. Lok, J. Zhao, and P. J. Zhao, "Oscillation elimination in the Hopkinson bar apparatus and resultant complete dynamic stress-strain curves for rocks," *International Journal of Rock Mechanics and Mining Sciences*, vol. 37, no. 7, pp. 1055–1060, 2000.

[6] F. Gong, X. B. Li, X. Liu, and Z. Jian, "Experimental study of dynamic characteristics of sandstone under one-dimensional coupled static and dynamic loads," *Chinese Journal of Rock Mechanics and Engineering*, vol. 29, no. 10, pp. 2076–2085, 2010.

[7] J. J. Zhu, X. B. Li, F. Q. Gong, S. M. Wang, and W. He, "Experimental test and damage characteristics of sandstone under uniaxial impact comprehensive loads," *Journal of Central South University*, vol. 43, no. 7, pp. 2701–2707, 2012.

[8] X. L. Yang, X. Y. Yuan, Z. Wu, and C. -D. Su, "The experimental study on mechanical properties of blast damaged rock," *Chinese Journal of Rock Mechanics and Engineering*, vol. 20, no. 4, pp. 436–439, 2001.

[9] J. Z. Liu, J. Y. Xu, X. C. Lu, L. Zang, and Z. Wang, "Experimental study on dynamic mechanical properties of amphibolites under impact comprehensive loading," *Chinese Journal of Rock Mechanics and Engineering*, vol. 28, no. 10, pp. 2113–2121, 2009.

[10] Y. You, E. Li, Y. Tan, J. Duan, and M. Yang, "Analysis on dynamic properties and failure characteristics of salt rock based on energy dissipation principle," *Chinese Journal of Rock Mechanics and Engineering*, vol. 36, no. 4, pp. 843–851, 2017.

[11] R. S. Yang, W. Y. Li, S. Z. Fang, Y. Zhu, and Y. l Li, "Experimental study on impact dynamic characteristics of layered composite rocks," *Chinese Journal of Rock Mechanics and Engineering*, vol. 38, no. 9, pp. 1747–1757, 2019.

[12] J. F. Jin, Y. Yang, Z. X. Liao, X. Yu, and Y. . l. Zhong, "Effect of dynamic load and geo-stress on response characteristics of rock," *Chinese Journal of Rock Mechanics and Engineering*, vol. 40, no. 10, pp. 1990–2002, 2021.

[13] Y. Chen, H. Wu, H. Pu et al., "Investigations of damage characteristics in rock material subjected to the joint effect of cyclic loading and impact," *Energies*, vol. 13, 2020.

[14] Q. Zheng, H. Hu, A. Yuan et al., "Impact Dynamic Properties and Energy Evolution of Damaged Sandstone Based on Cyclic Loading Threshold," *Shock and Vibration*, vol. 2020, pp. 1–12, 2020.

[15] S. Gong, Z. Wang, L. Zhou, and W. Wang, "Influence of Cyclic Impact Loading and Axial Stress on Dynamic Mechanical Properties of Burst-Prone Coal," *Shock and Vibration*, vol. 2021, pp. 1–10, 2021.

[16] N. Wu and J. Fu, "Research on the impact response and chaos characteristics in the dynamic damage evolution process of concrete material," *Construction and Building Materials*, vol. 262, no. 11, Article ID 120921, 2020.

[17] K. Duan, Y. Ji, W. Wu, and C. Y. Kwok, "Unloading-induced failure of brittle rock and implications for excavation-induced strain burst," *Tunnelling and Underground Space Technology*, vol. 84, no. 2, pp. 495–506, 2019.

[18] A. Cao, G. Jing, Y.-l. Ding, and S. Liu, "Mining-induced static and dynamic loading rate effect on rock damage and acoustic emission characteristic under uniaxial compression," *Safety Science*, vol. 116, pp. 86–96, 2019.

[19] K. Zhao, X. Yu, Y. Zhou, Q. Wang, J. Wang, and J. Hao, "Energy evolution of brittle granite under different loading rates," *International Journal of Rock Mechanics and Mining Sciences*, vol. 132, no. 7, Article ID 104392, 2020.

[20] C. A. Yan, B. Jz, A. Zl, and D. A. Rong, "Experimental investigation on the crack propagation behaviors of sandstone under different loading and unloading conditions," *International Journal of Rock Mechanics and Mining Sciences*, vol. 130, 2020.

[21] F. Wang, H. Wang, Y. Xu, B. Cheng, and Q. Wang, "Analysis of energy dissipation characteristics of damaged sandstone under impact load," *Shock and Vibration*, vol. 2021, pp. 1–10, 2021.

[22] Y. Luo, G. Wang, X. Li et al., "Analysis of energy dissipation and crack evolution law of sandstone under impact load," *International Journal of Rock Mechanics and Mining Sciences*, vol. 132, no. 3, Article ID 104359, 2020.

[23] F. Gong, H. Jia, Z. Zhang, J. Hu, and S. Luo, "Energy dissipation and particle size distribution of granite under different incident energies in SHPB compression tests," *Shock and Vibration*, vol. 2020, 2020.